Available online at www.sciencedirect.com

ScienceDirect

Energy Procedia 150 (2018) 21–27

Energy Procedia

www.elsevier.com/locate/procedia

12th International Photovoltaic Power Generation and Smart Energy Conference & Exhibition (SNEC 2018)

Device Parameter Extraction for Loss Analysis of Silicon Solar Cells Based on Intelligent Model Fitting

Jian Wei HO[a,*], Johnson WONG[b], Percis Teena CHRISTOPHER SUBHODAYAM[a], Kwan Bum CHOI[a], Divya ANANTHANARAYANAN[a], Samuel RAJ[a], Armin G. ABERLE[a]

[a] *Solar Energy Research Institute of Singapore, National University of Singapore, 117574, Singapore*
[b] *Aurora Solar Technologies Inc., North Vancouver, V7P 3N4, Canada*

Abstract

A fully automated and rigorous loss analysis routine that provides a breakdown of the loss components occurring in silicon solar cells is presented in this work. The routine combines large-area two-dimensional modeling and smart auto-fitting routines with luminescence imaging. This allows the spatially resolved information in luminescence images to be analyzed to extract recombination parameters partitioned by regions (e.g. wafer edge, under metal contacts, over passivated areas), as well as the spatial distribution of contact resistance. After these cell parameters have been extracted, a loss analysis of open-circuit voltage can be performed by simulating the open-circuit condition and examining the various recombination currents, and a loss analysis of fill factor can be performed by successively turning off the effects of factors that degrade it in simulation. The technique is demonstrated on a multicrystalline silicon PERC solar cell.

© 2018 The Authors. Published by Elsevier Ltd.
This is an open access article under the CC BY-NC-ND license (https://creativecommons.org/licenses/by-nc-nd/4.0/)
Selection and peer-review under responsibility of the scientific committee of the 12th International Photovoltaic Power Generation and Smart Energy Conference & Exhibition (SNEC 2018).

Keywords: Silicon wafer solar cells; loss analysis; luminescence imaging; model fitting; multivariate regression

* Corresponding author. Tel.: +65 6516 8987; fax: +65 6775 1943.
E-mail address: jw.ho@nus.edu.sg

1876-6102 © 2018 The Authors. Published by Elsevier Ltd.
This is an open access article under the CC BY-NC-ND license (https://creativecommons.org/licenses/by-nc-nd/4.0/)
Selection and peer-review under responsibility of the scientific committee of the 12th International Photovoltaic Power Generation and Smart Energy Conference & Exhibition (SNEC 2018).
10.1016/j.egypro.2018.09.012

1. Introduction

Understanding and quantification of the various power losses occurring within a completed solar cell is instrumental to any efficiency improvement program. This allows the identification of performance limiting aspects, such that actions targeting solar cell design and/or processing can be carried out. While there are numerous reports in literature analyzing Si solar cells [1-6], most of these do not address the fact that solar cells are large area devices with spatial dependence in parameters. This can arise due to spatial non-uniformities during processing or spatial variation in material properties itself especially in the case of multicrystalline Si solar cells. Various excellent 2D/3D device simulators (e.g. Sentaurus [7], ATLAS [8], Quokka [9], etc) are available for modeling Si solar cells and which have been adapted for performing loss analysis [2]. However, there remains a general lack of a systematic and streamlined approach that combines spatially resolved measurements and a 2D device model for loss analysis. In this work, we build upon previous work by Wong et alia [10, 11] and present a practical and systematic means to do so with a focus on solar cell non-uniformity. The method combines large-area two-dimensional modelling via a vast network of diodes and smart auto-fitting routines with luminescence imaging and other standard measurements. This has the unique capability of extracting recombination parameters, as well as contact resistance fast and non-destructively. The approach does not require specially prepared test structures and can be directly applied to finished Si wafer solar cells to discern general component losses in voltage and fill factor.

2. Experimental and Modeling Details

Multicrystalline Si wafer solar cells are exemplary in illustrating the spatial variation encountered in practice. In this work, a 156 mm by 156 mm commercial p-type multicrystalline PERC Si solar cell is employed as the subject for loss analysis. The steps are listed below.

A. Measurement of solar cell characteristics
B. Generation of solar cell model
C. Automated multivariate regression of cell model parameters to achieve least squares fit of simulated luminescence images to experimental images
D. Loss analysis (voltage & fill factor)

2.1. Measurement of Solar Cell Characteristics

In order to realistically describe the solar cell under test for modeling, the following characterization is performed.

- Dimensional measurements of the metallization grid and wafer size to physically define the cell.
- I-V characterization in the dark and under 1-Sun condition under a Class AAA Xe lamp solar simulator to compute the shunt resistance R_{sh} in addition to the J_{sc}, V_{oc} and fill factor [12].
- Busbar-to-busbar and line resistance measurements to determine the metallization finger and busbar sheet resistance. The emitter sheet resistance, if unknown, should be determined as appropriate by e.g. transmission line measurement (TLM) of cut sections of the cell.
- Luminescence imaging to obtain spatially resolved information. Open-circuit Suns-PL and Suns-V_{oc} are performed at incident light intensities from 3.6 Suns to 0.04 Suns. In addition, bias PL imaging is performed at the following conditions:
    (i) Reverse bias 0.5 V at 1 Sun;
    (ii) Current extraction at $0.25I_{sc}$ value under 1 Sun;
    (iii) Current extraction at $0.75I_{sc}$ value under 1 Sun;
    (iv) Current extraction at I_{sc} value under 2 Suns;
    (v) Current injection at I_{sc} value in the dark (electroluminescence).

2.2. Generation of Solar Cell Model

The parameters measured in the prior section are inputs to a solar cell device simulator called Griddler. This is a 2D finite element modeling program capable of simulating the voltage distribution across the cell plane [10, 11]. Here

the solar cell is modelled as a vast network of interconnected unequal diodes and resistors [13] (two-diode model), and enables the distributed nature of recombination and resistive effects over the solar cell expense to be captured. As such Griddler is especially suited for modelling experimentally acquired luminescence images with strong spatial dependence. A free version of the program is available for download from Ref. [14]. The Griddler interface is shown in Fig. 1. The interface presents an easy means to input properties of the solar cell for simulation.

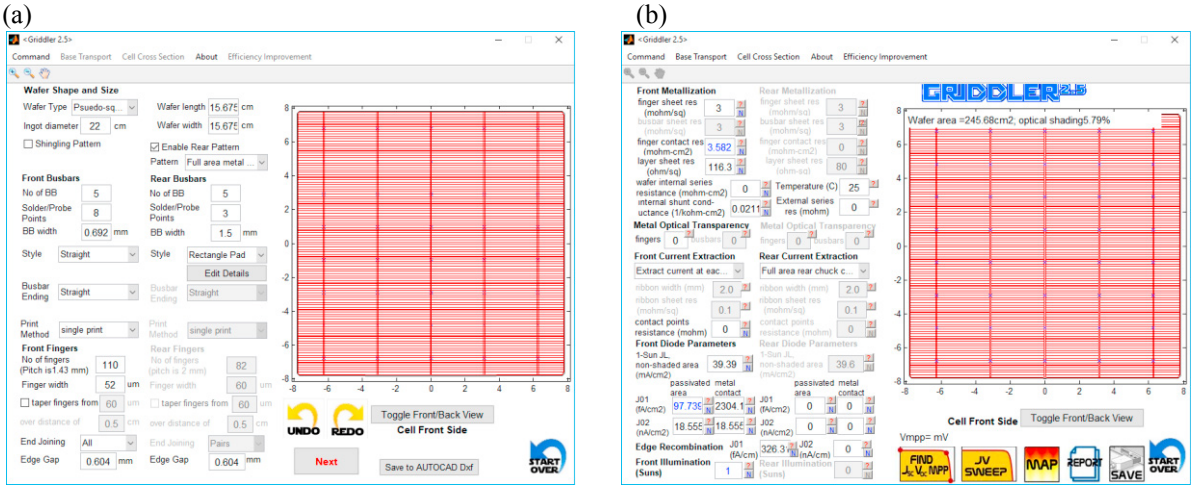

Fig. 1. Griddler interface for specifying (a) dimensional attributes and (b) other attributes.

2.3. Intelligent fitting of device model

The generated Griddler model is fitted to the series of acquired luminescence images specified in Section 2.1 via a multivariate regression routine implemented in a special version of Griddler called Griddler AI. The choice of the luminescence images plays a crucial role in the initial voltage calibration of the PL images and the computation of the spatially variable J_0. This is briefly described as follows.

The PL intensity $I(x,y)$ for a position (x, y) may be expressed as

$$I(x,y) = C(x,y)\exp\frac{V(x,y)}{V_T} + B(x,y)I_L \tag{1}$$

where $C(x,y)$ and $B(x,y)$ are position dependent calibration constants, $V(x,y)$ is the junction voltage at (x,y), V_T is the thermal voltage, and I_L is the illumination intensity [15].

The calibration constants are allowed to vary spatially to take into account the spatial variation in cell properties. The method for determining $C(x,y)$ and $B(x,y)$ follows that described by Glatthaar et alia [15]. $B(x,y)$ is typically small and can be neglected. If required, $B(x,y)$ can be obtained with image (i) in Section 2.1.

To determine $C(x,y)$, the open-circuit PL image at the lowest illumination intensity (0.04 Suns) is used. Under this condition, lateral voltage gradients is small such that $V(x,y)$ can be assumed to be equal to the measured open-circuit voltage, thereby allowing $C(x,y)$ to be computed.

The *relative* spatial distribution of $J_0(x,y)$ is then determined analytically with images (ii) and (iii) employing a terminal-connected diode model described by Glatthaar et alia [15]. In their model, the large-area solar cell is represented by numerous diodes each connected to the terminal via a series resistance $R(x,y)$. While $R(x,y)$ is determined simultaneously, these are not specifically utilized in the Griddler AI fitting process.

With the determination of $C(x,y)$ and the normalized $J_0(x,y)$ distribution, Griddler AI is instructed to simulate the luminescence images under the respective conditions, i.e. open-circuit PL images, and bias PL images (iv) and (v) as specified in Section 2.1. The fitting parameters include the saturation current densities at the passivation region (namely J_{01} and J_{02}), metal ($J_{01,met}$), edge (J_{01}) and contact resistance. As only the finished cell is analyzed, the fitting parameters contain the lumped contributions of both the front and rear sides. Cell intermediates, such as one-side metallized samples would permit a finer separation of the recombination parameters. Nonetheless, the reported approach still provides convenient analysis for end-of-the-line cells. Among the fitting parameters, the passivated region J_{01} and contact resistance are allowed to take on spatial distributions. The latter is defined in terms of a 5 by 5 square array with values at other positions within the cell plane computed by linear interpolation. Regions of interest (ROIs) are defined within each luminescence image as shown in Fig. 2.

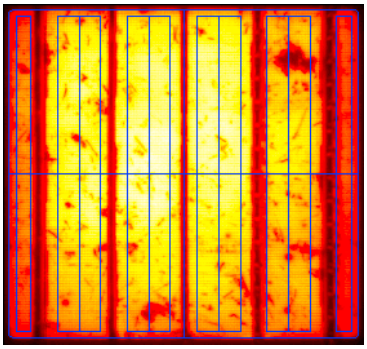

Fig. 2. Regions of interest (rectangular blue boxes) defined within a luminescence image used for computing goodness of fit in Griddler AI. (Alignment crosshair is also shown.)

Using a multivariate regression routine, Griddler AI iteratively seeks the best set of fitting parameters that yield the least root mean square (RMS) error associated with the luminescence at ROIs defined as follows.

$$RMS\ error = \sqrt{\sum_{all\ images}\sum_{all\ ROIs} kT \ln\left[\frac{average\ simulated\ luminescence\ in\ ROI}{average\ measured\ luminescence\ in\ ROI}\right]^2} \quad (2)$$

3. Results and Discussion

3.1. Fit results

The Griddler AI fitting process ultimately yields a Griddler model that best fits the luminescence images. Tables 1 and 2 show the values of the fitted parameters. Agreement between the measured and simulated I-V characteristics is generally good, although Griddler AI tends to underestimate the fill factor. The reason for this is still under investigation. The spatial distribution of the contact resistance and the passivated region J_{01} is shown in Fig. 3. Contact resistance is notably higher in the central section and indicates a need to examine process spatial non-uniformity. The coarse spatial resolution is a consequence of the cell being evaluated as a 5 by 5 square grid. In addition to non-uniformity caused by crystal grain orientation, there is significantly higher passivated region J_{01} at the cell periphery.

Table 1. I-V characteristics

	Measured	Simulated
V_{oc} (mV)	657.2	655.0
J_{sc} (mA/cm^2)	37.11	37.11
Fill factor (%)	80.09	79.60
Efficiency (%)	19.53	19.35

Table 2. Results of fitting

Griddler fitting parameter	Best-fit value
Passivated region J_{01} (fA/cm^2)	97.74 (average)
Lumped J_{02} (Passivated region & metal induced) (nA/cm^2)	18.56
Metal induced J_{01} (fA/cm^2)	2304.20
Edge J_{01} (fA/cm)	326.32
Peripheral J_{01} (fA/cm^2)	98.74
Contact resistance (mΩ.cm^2)	3.582 (average)

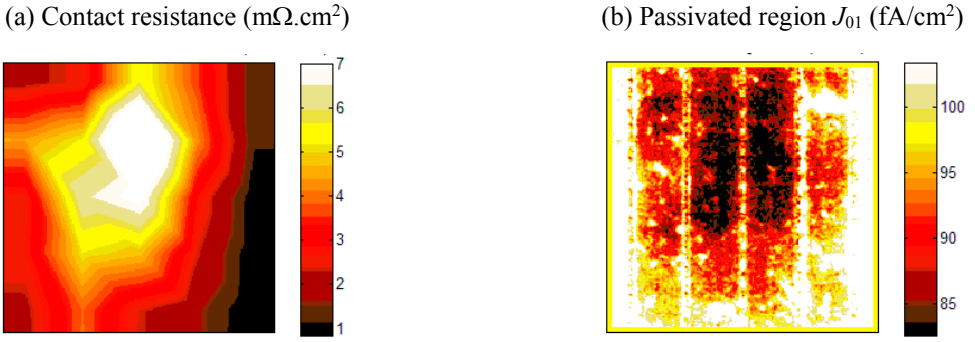

Fig. 3. Spatial distribution of the (a) contact resistance, and (b) passivated region J_{01} obtained via the Griddler AI fitting process.

The goodness of fit for the multicrystalline Si PERC solar cell under analysis can be examined by comparing the experimentally acquired and the corresponding Griddler AI simulated luminescence images (Fig. 4). The difference in voltages between the acquired and fitted images is small at within 1-3 mV, indicating a good fit.

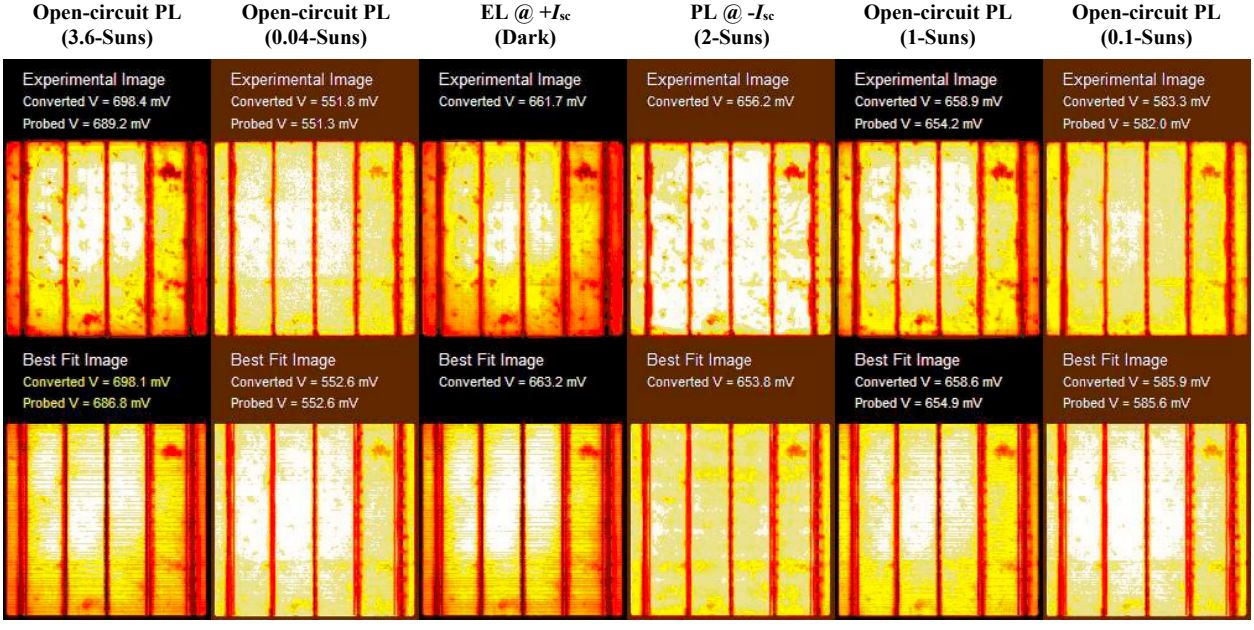

Fig. 4. Acquired luminescence images of the multicrystalline Si solar cell (top row) and the corresponding images simulated by Griddler AI (bottom row). "+I_{sc}" refer to current injection at the I_{sc} value while "-I_{sc}" refer to current extraction at the I_{sc} value.

It is important to note that the technique, when used with just the finished cell, is unable to discriminate between the front and rear side parameters. The front and rear side saturation current densities are lumped and divided into metallized region and non-metallized (non-front-grid) region. Similarly, the fitted contact resistance would contain contributions from both the front and rear contacts. A homogenous rear surface might make for a case of easier analysis (assumed in the case of Al-BSF) since spatial non-uniformity can be attributed to the front side and the contribution of the rear, if known, can be easily subtracted out. Nonetheless, for the case of a patterned rear side (e.g. PERC cell, or cases where the rear uniformity is not known with confidence), the extracted parameters still provide a good gauge of the effective spatial distribution of the contact resistance and J_{01} contributed by both the front and rear sides. A better separation of device parameters (for PERC and bifacial solar cells) is possible if other specially prepared samples are input for analysis. This is the topic of a future publication.

3.2. Voltage and fill factor loss analysis

Griddler is based on two-diode modeling with diode ideality factors n=1 and n=2. The spatially distributed nature of analysis in the approach allows the two-diode model to be applied in the metallized region and non-metallized (non-front-grid) region. With the fitted model, it is then straightforward to use Griddler to compute the voltage and fill factor losses occurring within the solar cell. Voltage losses can be quantified in terms of the J_0 contribution at 1-Sun open-circuit condition as shown in the pie chart of Fig. 5(a). As can be seen, the contribution to total recombination current by the passivated region (non-front grid) n=2 source is notable, exceeding half that of the n=1 source at the passivated region. In addition, metal-induced recombination comprises a significant portion of the voltage losses and efforts should be directed towards reducing it.

Fill factor (FF) losses due to resistive effects are calculated by simulating the resistive power dissipation at the maximum power point [16]. It is important to note that the FF loss to the rear metal is negligible since I-V testing (and hence modelling) is performed with it shorted to the conductive copper chuck. Fill factor losses due to recombination effects are computed in a similar manner as that of voltage losses by successively turning off each recombination source. Figure 5(b) shows the waterfall diagram depicting the component losses. n = 2 recombination is significant, causing ~2.6% loss in FF. This has been frequently attributed to Shockley-Read-Hall recombination in the space charge regions of the cell, injection dependent lifetime behavior, and would deserve some attention in efficiency improvement plans.

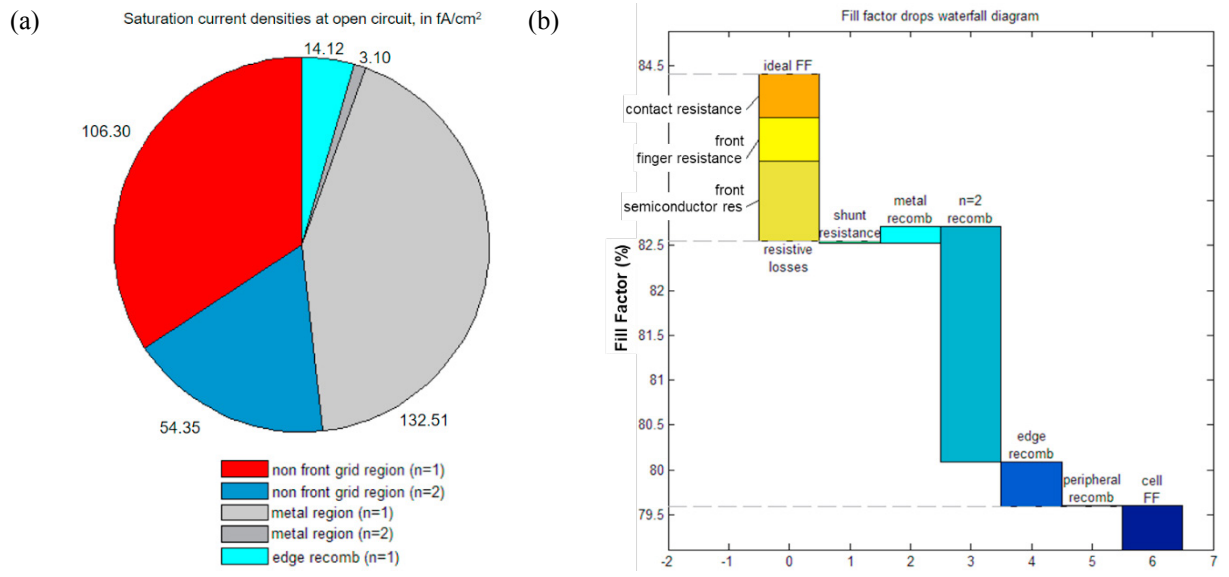

Fig. 5. (a) Saturation current densities at open-circuit attributable to various recombination sources, (b) Component fill factor losses arising from various mechanisms. n=1 and n=2 refers to the diode ideality factors used in two-diode modeling in Griddler.

4. Conclusion

In this work, a systematic and rigorous loss analysis technique for silicon solar cells is presented, using a multicrystalline Si PERC cell as a test vehicle. The technique combines large-area two-dimensional modeling (in a finite element modelling program called Griddler) and smart auto-fitting routines (implemented in Griddler AI) with luminescence imaging. The technique takes into account spatial non-uniformities which is especially relevant since solar cells are large-area devices and subject to spatially non-uniform material properties and processes. Another key advantage is that only the completed cell is required. The method has the unique capability of extracting recombination parameters traced to different regions of the cell, as well as the spatial distribution of contact resistance. A breakdown of the loss components occurring in silicon solar cells can be easily generated for identification of performance limiting aspects, such that actions targeting solar cell design and/or processing can be carried out.

Acknowledgements

The Solar Energy Research Institute of Singapore (SERIS) is a research institute at the National University of Singapore (NUS). SERIS is supported by the National University of Singapore (NUS), National Research Foundation Singapore (NRF) and the Singapore Economic Development Board (EDB).

References

[1] B. Rolf, D. Thorsten, P. Robby, K. Christopher, M. Agnes, and W. Daniel, "Breakdown of the efficiency gap to 29% based on experimental input data and modeling," *Progress in Photovoltaics: Research and Applications,* vol. 24, no. 12, pp. 1475-1486, 2016.
[2] N. Wehmeier *et al.*, "21.0%-efficient screen-printed n-PERT back-junction silicon solar cell with plasma-deposited boron diffusion source," *Solar Energy Materials and Solar Cells,* vol. 158, Part 1, pp. 50-54, 12// 2016.
[3] H. Huang *et al.*, "20.8% industrial PERC solar cell: ALD Al2O3 rear surface passivation, efficiency loss mechanisms analysis and roadmap to 24%," *Solar Energy Materials and Solar Cells,* vol. 161, no. Supplement C, pp. 14-30, 2017/03/01/ 2017.
[4] J. Sheng *et al.*, "Development of a large area n-type PERT cell with high efficiency of 22% using industrially feasible technology," *Solar Energy Materials and Solar Cells,* vol. 152, no. Supplement C, pp. 59-64, 2016/08/01/ 2016.
[5] B. Lim, T. Brendemühl, T. Dullweber, and R. Brendel, "Loss Analysis of n-Type Passivated Emitter Rear Totally Diffused Back-Junction Silicon Solar Cells with Efficiencies up to 21.2&#x0025," *IEEE Journal of Photovoltaics,* vol. 6, no. 2, pp. 447-453, 2016.
[6] M. Müller *et al.*, "Loss analysis of 22% efficient industrial PERC solar cells," *Energy Procedia,* vol. 124, pp. 131-137, 2017/09/01/ 2017.
[7] Synopsys. (2018). *Sentaurus Device: An advanced multidimensional (1D/2D/3D) device simulator*. Available: https://www.synopsys.com/silicon/tcad/device-simulation/sentaurus-device.html
[8] Silvaco. (2018). *ATLAS*. Available: https://www.silvaco.com/products/tcad/device_simulation/atlas/atlas.html
[9] A. Fell, "A Free and Fast Three-Dimensional/Two-Dimensional Solar Cell Simulator Featuring Conductive Boundary and Quasi-Neutrality Approximations," *IEEE Transactions on Electron Devices,* vol. 60, no. 2, pp. 733-738, 2013.
[10] J. Wong, R. Sridharan, and V. Shanmugam, "Quantifying edge and peripheral recombination losses in industrial silicon solar cells," *IEEE Transactions on Electron Devices,* vol. 62, no. 11, pp. 3750-3755, 2015.
[11] J. Wong, S. Raj, J. W. Ho, J. Wang, and J. Lin, "Voltage Loss Analysis for Bifacial Silicon Solar Cells: Case for Two-Dimensional Large-Area Modeling," *IEEE Journal of Photovoltaics,* vol. 6, no. 6, pp. 1421-1426, 2016.
[12] A. G. Aberle, W. Zhang, and B. Hoex, "Advanced loss analysis method for silicon wafer solar cells," *Energy Procedia,* vol. 8, pp. 244-249, 2011/01/01/ 2011.
[13] J. Wong and M. A. Green, "From junction to terminal: Extended reciprocity relations in solar cell operation," *Physical Review B,* vol. 85, no. 23, p. 235205, 06/25/ 2012.
[14] SERIS. (2018). *Griddler 2.5: The Handy Solar Cell Simulator*. Available: http://www.seris.nus.edu.sg/activities/griddler-2.5.html
[15] M. Glatthaar *et al.*, "Evaluating luminescence based voltage images of silicon solar cells," *Journal of Applied Physics,* vol. 108, no. 1, p. 014501, 2010/07/01 2010.
[16] A. Khanna, T. Mueller, R. A. Stangl, B. Hoex, P. K. Basu, and A. G. Aberle, "A Fill Factor Loss Analysis Method for Silicon Wafer Solar Cells," *IEEE Journal of Photovoltaics,* vol. 3, no. 4, pp. 1170-1177, 2013.